ST open

RESEARCH ARTICLE

Stochastic gravitational-wave background on large cosmological scales

Tamara Rom

University of Split, Faculty of Science, Split, Croatia

Correspondence to:
Tamara Rom
University of Split, Faculty of Science, Rudera Boškovića 33, 21000 Split, Croatia
trom@pmfst.hr

Cite as:
Rom T. Stochastic gravitational-wave background on large cosmological scales. ST-OPEN. 2023; 4: e2023.2111.12.

DOI:
https://doi.org/10.48188/so.4.2

Aim: To formulate a model capable of distinguishing astrophysical from primordial gravitational-wave signals.

Methods: We used a biased tracer formalism valid on large cosmological scales to introduce modeling basics and connected black holes as sources of gravitational wave signal with dark matter.

Results: By deriving the model and using the online tool Code for Anisotropies in the Microwave Background (CAMB), we produced the matter power spectrum and used it to construct the gravitational-wave power spectra as a linear biased tracer. The spectra were generated for different Hubble constants and bias parameter values, showing the difference in the amplitude and scale dependence of the spectra.

Conclusion: Gravitational-wave background signals can be used as complementary cosmological probes in data from future gravitational-wave space detectors like Laser Interferometer Space Antenna (LISA) and others.

Keywords: gravitational waves; stochastic background; dark matter; bias; tracers; power spectrum

Introduction

The Universe contains baryonic matter and other unknown ingredients such as dark matter and dark energy. We currently know that there is around 5% of visible matter, 23% of dark matter, and 68% of energy as a cosmological constant or some other dark energy [1]. There are also gravitational waves (GWs) [2-5] creating a stochastic gravitational-wave background (GWB). Our Universe started in a Big Bang and is approximately 13.7 billion years old; its current temperature is around 2.73 K [5-7]. The Big Bang paradigm relies on observations derived from the Hubble diagram, temperature and polarization anisotropies of the cosmic microwave background, nucleosynthesis, and large-scale structure (LSS) tests – along with several ingredients outside of the Standard Model of particle physics: dark matter and dark energy (which dominate the universe's energy reserves) and

a mechanism generating small initial perturbations out of which structure formed, the dominant one being inflation [1].

Stochastic gravitational-wave background

Gravitational waves

The solving of Einstein's theory of General Relativity field equations [8] allowed for numerous phenomena such as black holes, gravitational lensing, and GWs to be predicted. GWs are ripples in the fabric of spacetime, which contracts or expands depending on their movement [2]. They have various sources – for example, they can be produced in a binary system of two stars orbiting each other. GWs carry away angular momentum and energy from the aforementioned binary system which can be indirectly detected, as R. Hulse and J. Taylor did while observing the pulsar PSR 1913+16 [3]. However, the first direct observation of GWs was made in 2015 from a binary black hole (BBH) merger by the Laser Interferometer Gravitational-Wave Observatory (LIGO) and Virgo collaboration, 100 years after the first theoretical prediction [4].

Motivation for studying stochastic background

A stochastic background of gravitational radiation is the superposition of gravitational-wave signals that are either too numerous or too weak to be individually detected [5]. They are unresolvable, unlike the large signal-to-noise ratio BBH and binary neutron star (BNS) merger signals [5]. After finding a stochastic background, the next step would be to create a GW analogue of the cosmic microwave background (CMB), which is a sky map of the temperature fluctuations, relative to T_0 = 2.73 K isotropic component in the CMB blackbody radiation [5-7]. CMB is a relic of electromagnetic radiation, dating back to approximately 380,000 years after the Big Bang [9]. It shows the *screenshot* of the density perturbations from the time of the last scattering of photons, which is a *seed* for LSS formation in the early universe [5]. Due to the different nature of gravitational interaction compared to that of the electromagnetic force, GWB would give information about the universe as it was about 10^{-22} seconds after the Big Bang [10]. Detecting cosmological GWB would therefore be extremely important, since it would be a window into the universe's earliest moments.

Different sources of gravitational-wave background

A stochastic background of gravitational radiation arises from an extremely large number of weak, independent, and unresolved gravitational-wave sources [11]. Such backgrounds could have been produced in the early universe from inflation, preheating dynamics, phase transitions, or cosmic strings and represent primordial or cosmological sources [11]. A GWB can also be produced from many unresolved astrophysical sources – for example, by combining the signal from the BBH and BNS mergers that evolved from stars (the so-called stellar-mass BBH) with BNS mergers [5, 11]. The binary system's mass is reciprocal to the frequency of the GW it produces; since stellar-mass BHs and NSs have relatively small masses, the signal they produce is at the high-frequency end (from around 10 Hz to a few

kHz) of the spectrum – this part of the spectrum can be detected by sensitive ground-based detectors like LIGO and Virgo [5, 10]. Greater mass systems produce lower-frequency GWs that are also expected to belong to the GWB and are potentially detectable by detectors such as the Laser Interferometer Space Antenna (LISA) space-based GW detector [5]. While differentiating astrophysical and gravitational-wave signals is important for our current and future ground-based and spaceborne GW detectors (and cosmological theories in general), a differentiation model has not yet been developed. We aimed to find a simple model capable of distinguishing astrophysical from primordial gravitational-wave signals.

Methods

There is no direct way of measuring the matter power spectrum, but many observables probe matter distribution indirectly [1]. Perhaps the most important observable is clustering, which uses galaxies or any astrophysical object as a *tracer* of the large-scale matter distribution [1]. Such observed distribution of galaxies, quasars, and clusters of galaxies – the LSS of the Universe – is one of the pillars of knowledge of the Universe's history [12]. If we discovered how the distribution of tracers is related to the underlying distribution of matter, we could better understand the composition of the Universe, properties of gravity, dark matter, dark energy, and the nature of producing the initial *seeds* of structure [12].

We used a relation known as *bias*, which connects luminous tracers (galaxies, voids, quasars, Lyman-α forest, 21cm hydrogen hyperfine structure transition lines, etc. [13, 14]) and matter, thus helping explain the observed LSS. In standard cosmological models, the initial conditions of the Universe's LSS come from quantum mechanical vacuum fluctuations – because of its origin, the precise initial conditions of the observable Universe cannot be deterministically predicted, therefore the theoretical treatment of the LSS is based on describing random fields [12]. Extracting anything besides qualitative information from the one-point function (mean of a random field) of galaxies is complicated, so cosmological conclusions have been inferred from the next-order statistic – the two-point correlation function and its Fourier transform (which is the power spectrum) [12]. The two-point correlation function gives the probability that two objects (e.g., galaxies) will be found within a fixed distance r of each other.

Considering an ansatz (i.e., the linear bias relation) as in Desjacques et al. [12]

$$\delta_{\mathrm{g}}(\vec{x}) \equiv \frac{n_{\mathrm{g}}(\vec{x})}{\bar{n}_{\mathrm{g}}} - 1 = b_1 \delta_{\mathrm{m}}(\vec{x}) = b_1 \left(\frac{\rho_{\mathrm{m}}(\vec{x})}{\bar{\rho}_{\mathrm{m}}} - 1 \right), \qquad (1)$$

$\delta_m(\vec{x})$ represents matter overdensity, $\bar{n}_{\mathrm{g}}$ is the mean comoving number density of galaxies, $\bar{\rho}_{\mathrm{m}}$ is the co-moving background matter density, and b_1 is a parameter called *bias* [12]. The linear relation of galaxies' density perturbation is "a guaranteed result at linear order in perturbations and on large scales" [1]. In this article, we focused on linear theory and relation. Equation 1 can be written as:

$$\delta_{\mathrm{g}}(\vec{x}) = b_1 \delta_{\mathrm{m}}(\vec{x}) \,. \tag{2}$$

The bias parameter, b_1, incorporates local physics (small-scale physics) such as galaxy mass, AGN feedback, metallicity, and others. While the bias parameter fully describes all the complexities of galaxy formation, this is a non-trivial result that heavily relies on gravity driving LSS formation. Most matter in the Universe is dark matter, which was key for connecting galaxies to matter (e.g., Equation 2) because galaxies *float* in halos of dark matter.

Equation 1 of the simple linear bias can be generalized as:

$$\delta \mathrm{g}(\vec{x}, \tau) \; = \sum_O b_O(\tau) O(\vec{x}, \tau) \,, \tag{3}$$

where O are operators, or statistical fields, that describe the dependency of a galaxy's density on its environment [12]. Furthermore, each operator was multiplied by a corresponding bias parameter b_O (a number at a fixed time) known as a local bias parameter [12]. Thus, it can be said that Equation 3 can describe local density distribution [12]. Equation 1 is an example of Equation 3 with $O = \delta_{\mathrm{m}}$ and $b_O = b_1$ [12].

Overdensities are useful because the correlation function whose Fourier transform is the power spectrum can be obtained. The correlation function only depends on the absolute distance from the objects due to the homogeneity and isotropy of our Universe [15]. The power spectrum is then observable using different detectors and sky surveys such as Planck or SDSS.

The correlation function, ξ, was mathematically defined as:

$$\xi(|\vec{r}|) = \left\langle \delta_{\mathrm{g}}(\vec{x}) \delta_{\mathrm{g}}(\vec{x}') \right\rangle = \frac{1}{V} \int d^3 \vec{x} \delta_{\mathrm{g}}(\vec{x}) \delta_{\mathrm{g}}(\vec{x} - \vec{r}) \,, \tag{4}$$

where $\vec{r} = \vec{x}' - \vec{x}$ [15]. The relationship to the power spectrum, was then derived as:

$$\xi(|\vec{r}|) = \int \frac{d^3 k}{(2\pi)^3} P(k) e^{i\vec{k} \cdot (\vec{x} - \vec{x}')} \,. \tag{5}$$

The matter power spectrum gives the difference between the local density and the so-called density contrast of the Universe as a function of scale. Its overall shape is best understood in terms of the linear perturbation theory analysis of the structure growth, which predicts to first order how the power spectrum grows. Although cosmic expansion is present on large scales, gravity's effect is still observable, allowing us to see structure growth as per the linear theory. In this regime, the power spectrum is sufficient to completely describe the density field [15]. One example of bias applied to GWs are sources originating from black holes. Black holes are mostly located in galaxies, and GWs come from black hole mergers. Since they are connected to the galaxies, this idea can be applied to bias for galaxies and matter and to GWs and galaxies as well.

Results

We obtained the following:

$$\delta_{\mathrm{GW}}(\vec{x}) = b_{\mathrm{GW}}\delta_{\mathrm{g}}(\vec{x}) = b_{\mathrm{GW}}b_1\delta_{\mathrm{m}}(\vec{x}) = c_1\delta_{\mathrm{m}}(\vec{x}), \tag{6}$$

where b_{GW} gives information, for example, on the type of galaxy or gravitational-wave source. Other factors are the same as in the previous section and c_1 is the combined bias parameter, containing both information from matter and gravitational-wave sources. To get the GW overdensity, we used the connection to the astrophysical sources, which are very well known. If an observable is derived that gives the whole overdensity, δ_{GW}, (astrophysical and primordial sources combined), any existing discrepancy between the theory and the data can be observed. If there were any discrepancies and our theory for the astrophysical data (modeled using matter overdensity with b_{GW} calculated in Equation 6) has already been checked, that would mean primordial GWs have been successfully detected. The correlation function of these overdensities is:

$$\xi_{\mathrm{GW}}(|\vec{r}|) = \langle \delta_{\mathrm{GW}}(\vec{x})\delta_{\mathrm{GW}}(\vec{x}')\rangle, \tag{7}$$

where $\vec{r} = \vec{x}' - \vec{x}$. However, several things must be assessed.

The correlation function for galaxies in the previous section was for the 3D distribution, yet GWs were defined over a 2D spherical distribution. It was necessary to derive the 3D GW density field and *reduce* it to a 2D projection on the sky because the relations for bias were used for the three dimensions only. The formalism and arguments shown for galaxies in Dodelson and Schmidt [1] were followed, where indices for galaxies were only substituted with the indices denoting GWs. Distance distribution $W(\chi)$ was defined as:

$$W(\chi) = \frac{1}{N_{\mathrm{GW}}}\frac{dN_{\mathrm{GW}}}{d\chi}, \tag{8}$$

defining Hubble rate [1]:

$$H(t) \equiv \frac{1}{a}\frac{da}{dt}. \tag{9}$$

The total comoving distance, χ, was then [1]:

$$\chi(t) = \int_t^{t_0}\frac{dt'}{a(t')} = \int_{a(t)}^{1}\frac{da'}{a'^2H(a')} = \int_0^z\frac{dz'}{H(z')}. \tag{10}$$

The projected overdensity, which gives a superposition of many slices of a 3D GW density field at different distances χ, weighted by the distance distribution, $\Delta_{GW}(\hat{\vec{n}})$ was obtained [1]:

$$\Delta_{\mathrm{GW}}(\hat{\vec{n}}) = \int_0^\infty d_\chi W(\chi)\delta_{\mathrm{GW,obs}}(\vec{x} = \hat{\vec{n}}\chi, \eta = \eta_0 - \chi)\,, \tag{11}$$

where η was a variable defined in Dodelson and Schmidt [1] as:

$$\eta(t) \equiv \int_0^t \frac{dt'}{a(t')}\,. \tag{12}$$

Now, we inserted the Fourier transform of $\delta_{\mathrm{GW,obs}}$, with the expansion of the exponential and several abbreviations, to get [1]:

$$\begin{aligned}\Delta_{\mathrm{GW}}(\hat{\vec{n}}) &= \int_0^\infty d\chi\, W(\chi) \int \frac{d^3k}{(2\pi)^3} e^{i\vec{k}\cdot\hat{\vec{n}}\chi}\, \delta_{\mathrm{GW,obs}}\left(\vec{k}, \eta(\chi)\right) \\ &= 4\pi \int \frac{d^3k}{(2\pi)^3} \sum_{lm} i^l Y_{lm}(\hat{\vec{n}}) Y^*_{lm}(\hat{\vec{k}}) \int_0^\infty d\chi\, W(\chi) j_l(k\chi)\, \delta_{\mathrm{GW,obs}}\left(\vec{k}, \eta(\chi)\right)\,,\end{aligned} \tag{13}$$

abbreviations $\eta(\chi) = \eta_0 - \chi$ and $\sum_{lm} \equiv \sum_{l=0}^{\infty} \sum_{m=-l}^{l}$ were used. The right-hand ones are basically the coefficients of $Y_{lm}(\hat{\vec{n}})$ [1]:

$$\Delta_{\mathrm{GW},lm} = 4\pi i^l \int \frac{d^3k}{(2\pi)^3} Y^*_{lm}(\hat{\vec{k}}) \int_0^\infty d\chi W(\chi) j_l(k\chi) \delta_{\mathrm{GW,obs}}(\vec{k}, \eta(\chi))\,. \tag{14}$$

As mentioned, by the argumentation and procedure from [1], the obtained angular power spectrum is:

$$\begin{aligned}C_{\mathrm{GW}}(l) = \frac{2}{\pi} \int k^2 dk \int_0^\infty d\chi W(\chi) j_l(k\chi) \int_0^\infty d\chi' W(\chi') j_l(k\chi') \\ \times P_{\mathrm{GW,obs}}\left(\vec{k}, \eta(\chi), \eta(\chi')\right)\,.\end{aligned} \tag{15}$$

Now, an assumption of looking at small scales as in Dodelson and Schmidt [1] was made, to simplify the equations, obtaining:

$$\frac{2}{\pi} \int k^2 dk j_l(k\chi) j_l(k\chi') P_{\mathrm{GW,obs}}\left(\vec{k}, \eta, \eta'\right)\,. \tag{16}$$

If $P_{\mathrm{GW,obs}}(\vec{k})$ were independent of k, it would give:

$$\frac{2}{\pi}\int k^2 dk j_l(k\chi) j_l(k\chi') = \frac{1}{\chi^2}\delta_{\mathrm{D}}^{(1)}(\chi-\chi')\,, \tag{17}$$

but that is not possible in reality [1]. For high l, the product of spherical Bessel functions very sharply peaks at $k\chi \approx k\chi' \approx \sqrt{l(l+1)} \approx l+1/2$ [1]. While $P_{\mathrm{GW,obs}}(\vec{k})$ varies slowly over the narrow range Δk over which the Bessel functions are nonzero, $\Delta k \sim 1/(l\chi)$, it can be approximated as constant [1]. This is the Limber approximation and it is usually very accurate at $l \gtrsim 20$ and very useful, since many sky surveys are limited to a smaller angle on the sky and not the whole field [1]. The core prediction of this approximation was

$$C_{\mathrm{GW}}(l) = \int \frac{d\chi}{\chi^2} W^2(\chi) P_{\mathrm{GW,obs}}\left(k = \frac{l+1/2}{\chi}, \mu_k = 0, \eta(\chi)\right), \tag{18}$$

which is easier to calculate than Equation 15 [1]. In the Limber approximation, $\chi = \chi'$ implies $\eta(\chi') = \eta(\chi)$, so Equation 18 only involves the equal-time power spectrum [1]. Physically, the Limber approximation equates to observing at small angles, $\theta \sim 1/l \ll 1$ [1].

The goal was to get to Equation 18 since an observable can be obtained from it, which is useful for detectors. However, the GW power spectrum element in that equation should be discussed. The $P_{\mathrm{GW,obs}}$ used in Equation 18 was defined as:

$$P_{\mathrm{GW,obs}}\left(\vec{k},\eta,\eta'\right) = c_1(\eta)c_1(\eta')P_{\mathrm{m}}\left(\vec{k},\eta,\eta'\right), \tag{19}$$

following from Equation 7. Next, P_{m} of dark matter can be stated explicitly as

$$P_{\mathrm{m}}\left(\vec{k},\eta,\eta'\right) = D_+(\eta)D_+(\eta')P_{\mathrm{m}}(\vec{k},0,0)\,, \tag{20}$$

where D_+ denotes the linear growth factor in the density and $P_{\mathrm{m}}(\vec{k},0,0)$ is commonly referred to as the primordial matter power spectrum related to the physics of inflation [15]. The simplest primordial matter power spectrum is the Harrison Zel'dovich spectrum, which characterizes $P_m(\vec{k})$ according to a power law, $P_m(\vec{k}) = Ak$, where A represents the scalar spectral index or the amplitude of fluctuations in the spectrum [15]. Notably, in the Harrison Zel'dovich spectrum, the power of k is not exactly equal to 1 but around 0.9 (Z. Vlah, personal communication, June 29, 2021). In **Figure 1**, the simulation of the matter power spectrum was shown for different values of the Hubble constant, H_0, that have been possible candidates for the true value of H_0. This simulation was made using the online tool Code for Anisotropies in the Microwave Background (CAMB) (Antony Lewis and Anthony Challinor, service of the The High Energy Astrophysics Science Archive Research Center (HEASARC)) and of the Astrophysics Science Division at National Aeronautics and Space Administration/Goddard Space Flight Center [16] that already provides various cosmological parameters. Specifically, cold dark matter was set at around 23% and baryonic matter around 5%, so the total matter was around 28%.

For this research, the simulation of the GW power spectrum was more important than the matter power spectrum; when the bias parameter equalled 1, it was identical to the matter power spectrum shown in **Figure 1**. However, for different bias parameter values, a different image was obtained. This difference was shown in **Figure 2** for when the Hubble constant H_0 equalled 67 km s^{-1} Mpc^{-1}. This value was chosen because (according to the latest Planck collaboration data) it is close to the current value of H_0 [17]. Bias in the legend means that

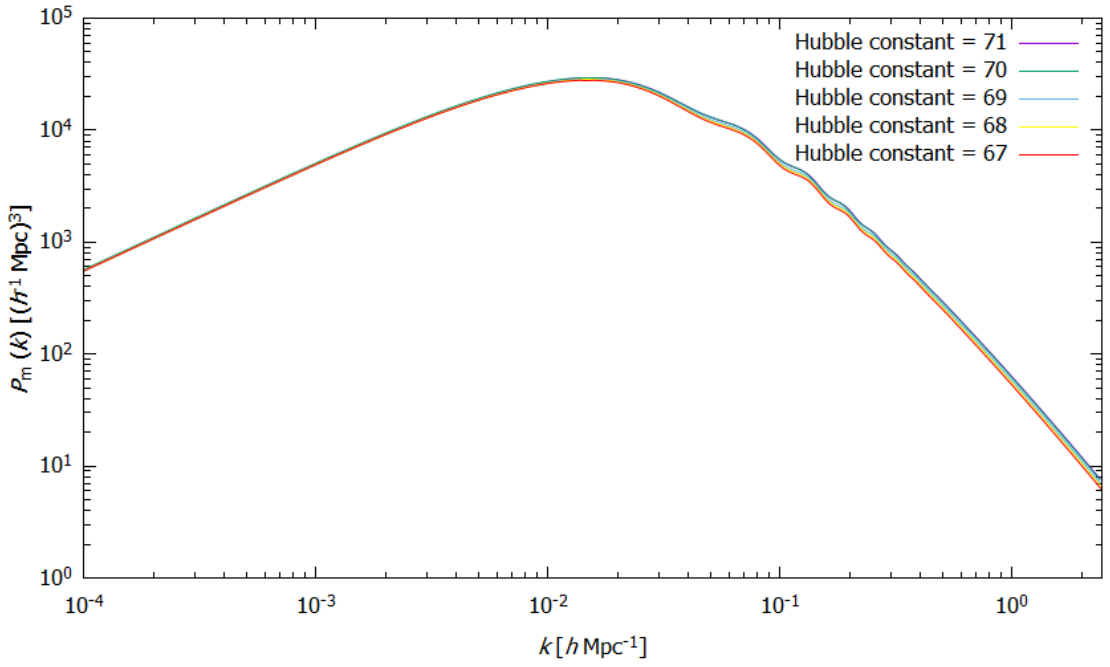

Figure 1. Simulation of the matter power spectrum using online tool Code for Anisotropies in the Microwave Background (CAMB). This figure also represents the gravitational wave power spectrum for the case when bias parameter equals to 1 according to the Equation 19. Link given at [16].

$c_1(\eta)c_1(\eta')$ = 1, $c_1(\eta)c_1(\eta')$ = 2, etc. The shape and the amplitude of this spectrum give astrophysical information, while only cosmological information can be obtained from the dependence on the dimensionless number h which defines the Hubble constant as H_0 = 100h $kms^{-1}Mpc^{-1}$.

Finally, the angular correlation function $w_{GW}(\theta)$ can be written [1]:

$$w_{\mathrm{GW}}(\theta) = \int_0^{\infty} \frac{dl}{2\pi} l C_{\mathrm{GW}}(l) J_0(l\theta) \ . \tag{21}$$

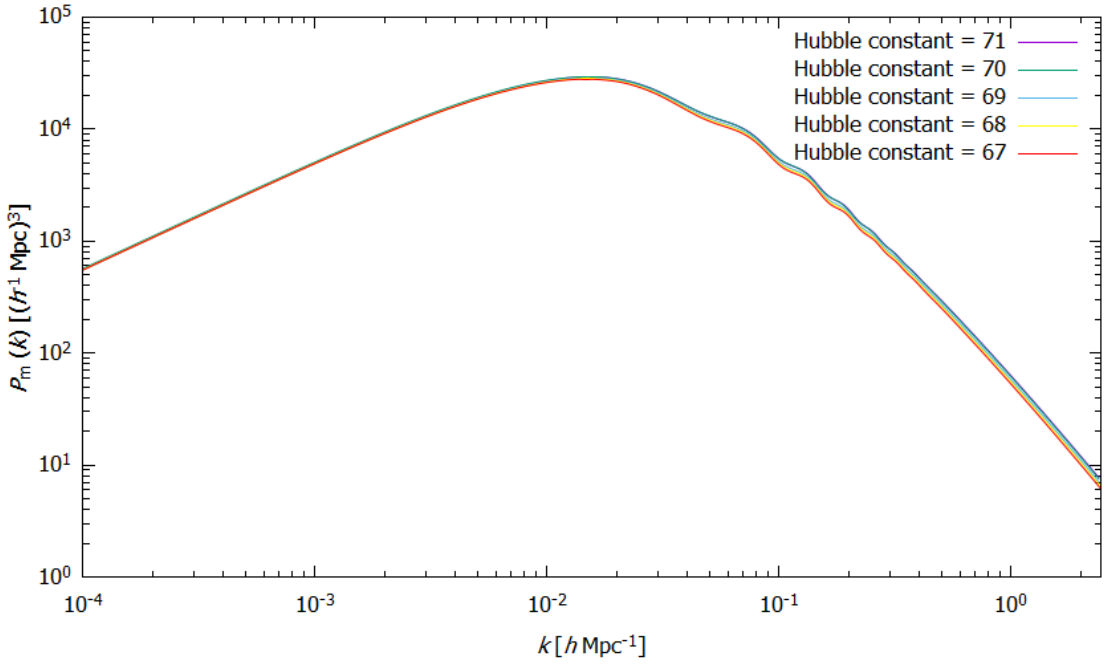

Figure 2. The simulation, using online tool Code for Anisotropies in the Microwave Background (CAMB), represented in Gnuplot, of the gravitational wave power spectrum derived from the matter power spectrum by multiplying with different values of bias.

Discussion

In this study, we reviewed the standard cosmological model, introduced basic cosmological terms, and categorized the astrophysical and cosmological gravitational-wave sources. Furthermore, we described the basics of bias galaxy tracers and the worth of using bias common to the LSS formation theory [12-14].

We applied the bias tracer method to GWs – i.e., we used traces of dark matter to outline where GWs should be *clumped* together or (inversely) used GWs as one of the tracers of dark matter fluctuations. This was done using bias formalism on variables such as a matter power spectrum and an angular power spectrum. Further work could be done by simulating Equation 18 for the data obtained from CAMB. The approach, describing the distribution of stochastic gravitational-wave sources as proportional to dark matter fluctuations, is a valid description on the largest cosmological scales, which is a limitation of this article.

Moreover, the tensor nature of GWs [2, 5] was simplified, and the approach of modelling the gravitational-wave source signals as scalar field was used, since most detectors used for detecting GWs do not detect their polarization [2, 18, 19]. This approach can be modified in future research to incorporate the tensor formalism. While this research was unique in its simplicity and approach, something similar, yet more sophisticated has been done by Bellomo et al. [20] and Shao et al. [21].

These results are useful for various GW detectors for a given matter and GW power spectrum, which are equivalent for the unity bias value. Bias values do not necessarily have

to be equal to unity – different spectrum amplitudes are expected for different types of biased tracers. However, the power spectrum's shape, i.e., the dependence on the wave number, can differ for different values of cosmological parameters like the Hubble constant, as was shown in **Figure 1** and **Figure 2**.

These results can be used to test current theories and data, such as inflation, Lambda-CDM model and gravity. For example, primordial waves have not yet been detected and are only speculated by the current cosmological theories of inflation [11, 22]. The power of applying the bias method to GWs lies in the fact, that once the correlations of stochastic GWB are measured, we can observe if they match the theoretical prediction obtained for astrophysical sources. Any unaccounted residual signal on a large scale would indicate the potential primordial GW origin.

This study is a primer in the area of stochastic GWBs on large scales. Future research could calculate another observable (e.g. Equation 18) and describe the stochastic GWB on smaller scales, but also include the GWs' tensor nature in the model.

Provenance: Submitted. This manuscript is based on the master's thesis by Tamara Rom at the University of Split, Faculty of science, and deposited in the Dabar repository (https://urn.nsk.hr/urn:nbn:hr:166:177584).

Peer review: Externally peer reviewed.

Received: 21 February 2022 / **Accepted:** 30 August 2022 / **Published online:** 21 April 2023.

Acknowledgements: The author wants to express the deepest gratitude to her mentor Dr Zvonimir Vlah for guidance during the preparation of her Master's thesis and his patience in explaining the study topic.

Funding: This research received no specific grant from any funding agency in public, commercial or not-for-profit sectors.

Authorship declaration: TR is the sole author of this study.

Competing interests: The author completed the ICMJE Unified Competing Interest form (available upon request from the corresponding author), and declares no conflicts of interest.

ORCID

Tamara Rom https://orcid.org/0000-0002-9076-2425

References

1. Dodelson S, Schmidt F. Modern Cosmology. 2nd ed. Amsterdam: Academic Press An imprint of Elsevier; 2021.
2. Gravitational wave [Internet]. Wikipedia. Wikimedia Foundation; 2022 [cited 2022Nov15]. Available from: https://en.wikipedia.org/wiki/Gravitational_wave
3. Hulse RA, Taylor JH. Discovery of a pulsar in a binary system. Astrophys J. 1975;195:51-3.
4. Abbott BP, Abbott R, Abbott TD, Abernathy MR, Acernese F, Ackley K, et al. Observation of Gravitational Waves from a Binary Black Hole Merger. Phys Rev Lett. 2016;116:061102-1-16.

5. Romano JD. Searches for stochastic gravitational-wave backgrounds. arXiv preprint arXiv:1909.00269. 2019, Available from: http://dx.doi.org/10.48550/ARXIV.1909.00269
6. Dicke RH, Peebles PJE, Roll PG, Wilkinson DT. Cosmic Black-Body Radiation. ApJ. 1965;142:414-19.
7. Penzias AA, Wilson RW. A Measurement of Excess Antenna Temperature at 4080 Mc/s. ApJ. 1965;142:419-21.
8. Einstein A. Die Feldgleichungen der Gravitation. Sitzungsberichte der Königlich Preussischen Akademie der Wissenschaften zu Berlin. 1915:844–847.
9. Planck and the cosmic microwave background [Internet]. European Space Agency [cited 2021Mar25]. Available from: https://www.esa.int/Science_Exploration/Space_Science/Planck/Planck_and_the_cosmic_microwave_background
10. Allen, B. The stochastic gravity-wave background: sources and detection. Relativistic Gravitation and Gravitational Radiation, Proceedings of the Les Houches School of Physics, held in Les Houches, Haute Savoie. 1997, January;26:373-418.
11. Jaranowski P, Krolak A. Analysis of gravitational-wave data. New York: Cambridge University Press; 2009.
12. Desjacques V, Jeong D, Schmidt F. Large-scale galaxy bias. Phys Rep. 2018:733:1-193.
13. Fujita T, Vlah Z. Perturbative description of biased tracers using consistency relations of LSS. JCAP. 2020;2020:1-59.
14. McDonald P, Roy A. Clustering of dark matter tracers: generalizing bias for the coming era of precision LSS. JCAP. 2009;2009:1-20.
15. Matter power spectrum [Internet]. Wikipedia. 2022 [cited 2022Dec3]. Available from: https://en.wikipedia.org/wiki/Matter_power_spectrum
16. NASA [homepage on the Internet]. Goddard Space Flight Center, Tools, CAMB [updated 2019 Apr 16; cited 2021 Jun 25]. Available from: https://lambda.gsfc.nasa.gov/toolbox/camb_online.html
17. Aghanim N, Akrami Y, Ashdown M, Aumont J, Baccigalupi C, Ballardini M et al. Planck 2018 results-VI. Cosmological parameters. A & A. 2020; 641, A6.
18. Philippoz LA. On the polarization of gravitational waves [dissertation]. University of Zurich: Faculty of Science; 2018.
19. Abbott BP, Abbott R, Abbott TD, Acernese F, Ackley K, Adams C et al. Search for Tensor, Vector, and Scalar Polarizations in the Stochastic Gravitational-Wave Background. Phys Rev Lett. 2018;120:201102-1-13.
20. Bellomo N, Bertacca D, Jenkins AC, Matarrese S, Raccanelli A, Regimbau T. CLASS_GWB: robust modeling of the astrophysical gravitational wave background anisotropies. JCAP. 2022;2022:1-30.
21. Shao X, Cao Z, Fan X, Wu S. Probing the Large-scale Structure of the Universe Through Gravitational Wave Observations. Res Astron Astrophys. 2022;22:015006(1-8).
22. Inflation (cosmology) [Internet]. Wikipedia. Wikimedia Foundation; 2022 [cited 2022Nov16]. Available from: https://en.wikipedia.org/wiki/Inflation_(cosmology)